

A contribution toward understanding DNS simulations of isotropic decaying turbulence using similarity theory

By HONGLU WANG,
JAMES R SONNENMEIER,
STEPHAN GAMARD AND WILLIAM K GEORGE

Turbulence Research Laboratory
State University of New York at Buffalo
Buffalo, NY 14260 USA

The equilibrium similarity theory of George(1992) is evaluated using several recent DNS simulations of isotropic decaying turbulence. The theory and data are found to be in remarkable agreement. Moreover, the theory is shown to be useful in clarifying the behavior of the simulations at very low and very high wavenumbers where resolution is generally a concern, and as well as when the simulations can be considered fully-developed.

1. Introduction

One of the most difficult problems in modern experiments and computer simulations of turbulence is to establish precisely the effect of boundaries and resolution. The primary reason for this is that, unlike many other problems in mechanics, there are no exact analytical solutions with which the computed results can be compared. This is especially true for the averaged properties where the closure problem of the averaged equations precludes any solution at all — at least solutions independent of the particular turbulence model selected. So the standard practice has been simply to vary both the domain and resolution until results are obtained which are believed to be independent of both. Unfortunately, because of the time and expense, this can not always be done.

A further complication is that all attempts to simulate turbulence (in both the computer and laboratory) require some time (or distance) for the starting transients to die off. Deciding exactly how long one has to wait to insure they have can be one of the most difficult parts of carrying out the effort. Minimizing this development time can be quite important to the overall success of the effort, since the end of the calculation (or experiment) might be contaminated by the saturation of the largest scales which continue to grow until they fill the domain, the so-called ‘box-size’ effect.

One way to gain confidence in the validity of experimental and numerical results is to plot the averaged quantities using non-dimensional variables. The collapse of computed (or measured) results in such variables can be a powerful indicator of the success or failure of the effort. This is especially true when the averaged equations and boundary conditions admit to similarity solutions. When such solutions exist there can be no doubt that the scaling represents real physics, so collapse of the data implies accuracy of the simulation.

A major problem with even this approach is that the validity of similarity solutions in turbulence have themselves been in doubt, at least until recently. For the decaying

isotropic turbulence considered here, the classical von Karman & Howarth(1938) analysis of has been long known to be inconsistent with the experimental data (cf. Comte-Bellot & Corrsin(1966)). At least part of the problem, however, was resolved by George(1992) who showed that these self-preserving solutions were based on assumptions which were too restrictive. In particular, it had previously been *assumed* that the triple moment correlations (or their counterpart in wavenumber space, the spectral energy transfer) were independent of the local Reynolds number, R_λ . This was, in fact, a direct consequence of the rather unique idea in turbulence that flows should be governed by *single length and velocity scales*; hence the term *self-preserving* solutions instead of *similarity*. When this self-preservation assumption was relaxed and the appropriate scale was determined from the governing equations using only an equilibrium hypothesis, a whole new class of similarity solutions was shown to be possible.

The new theory resolved many of the problems of the old theory in accounting for the experimental data. In addition it showed that the energy spectra could, in principle, retain an asymptotic dependence on the initial (or upstream) conditions. The prediction that the energy decayed as a power law ($u^2 \sim t^n$) had long been confirmed by experiment. Also the decay exponent in both experiments and DNS showed a sensitivity to initial conditions, exactly as predicted, as did the exact spectral shape. Most importantly, energy spectra normalized with u^2 and λ , the Taylor microscale, showed remarkable collapse over all wavenumbers when compared for fixed upstream (or initial) conditions. Although DNS simulations were in their infancy a decade ago, they were at least partly consistent with these results.

There were, however, several troubling aspects of the new theory. One was the prediction that the integral scale, L , and λ remained proportional throughout decay. While the velocity spectra from the experiments appeared to collapse for all wavenumbers with simply u^2 and λ , the ratio of L/λ showed a small but progressive deviation for the longitudinal integral scale. George argued that the experimental integral scales were too small because of the low frequency cutoff of the anemometers, as well as the fact that the largest scales of the flow were being influenced by the finite lateral dimensions of the tunnel. The latter effect is seldom discussed in either experiments and simulations, but clearly there must be some wavenumber below which an experiment or simulation is not a reasonable model of a homogeneous turbulence in an infinite domain — and it is only the latter for which the theory applies. The same trend is observed in recent DNS data, as shown in Figure 1. This data will be discussed in detail later.

Another troubling aspect of the new theory was the prediction of how the velocity derivative skewness varied with R_λ . On this point the theory and the experiments were in complete agreement, but the DNS results were not. In particular, the theory predicted that $SR_\lambda = \text{constant during decay for fixed upstream conditions}$. The constant depends on the upstream (or initial) conditions, and increases (in the experiments) with the grid Reynolds number. For the DNS simulations, however, the derivative skewness ($S < 0$) rapidly reached a minimum value, then slowly increased, opposite to the predicted behavior. Figure 2 shows plots of $-SR_\lambda$ versus time for the same two DNS simulations used above. Unlike the earlier results, these might asymptote to a constant. Even so, it is not obvious why the progression should be so slow.

Over the past decade there has been considerable development of massively parallel computers. This has greatly increased the size (in number of Fourier modes) and length (in time) of the DNS simulations. Now, for the first time there is reasonable agreement between most of the details of DNS isotropic simulations and experiments on grid turbulence, de Bruyn Kops & Riley(1998). Also, there is an increased understanding of the subtleties of equilibrium similarity, especially since it appears to describe more than just

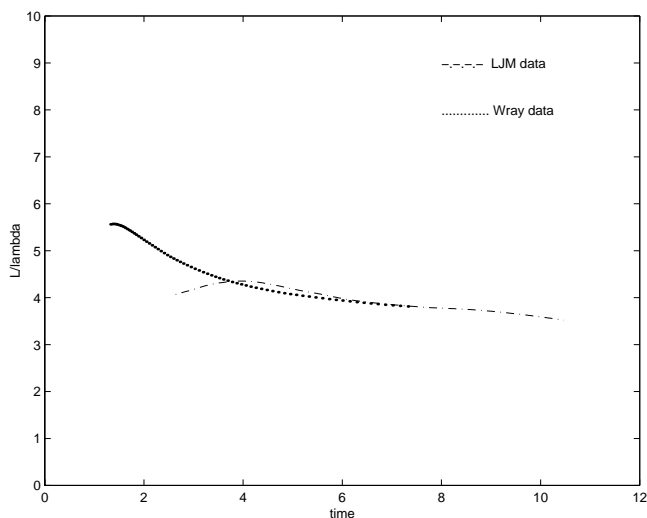
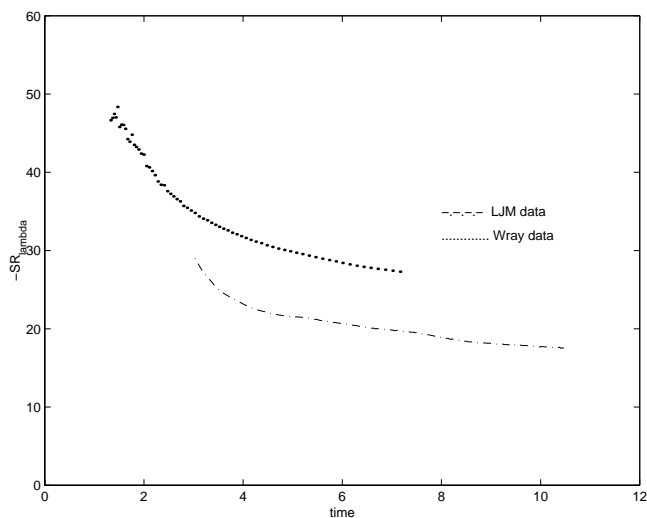


FIGURE 1. Ratio of integral scale to Taylor microscale (Wray and LJM data).

FIGURE 2. $-SR_\lambda$ from DNS (Wray and LJM data).

a few flows (George(1999)). Therefore it is appropriate and timely to re-visit the questions raised above, as well as the entire question of whether equilibrium similarity is an accurate description of the physics of isotropic decay.

In this paper the fundamental results of the George(1992) theory will be evaluated using two different DNS simulations. These were long-time calculations carried out with different initial spectra and different resolutions of the small scales. The theory will be seen to be generally confirmed. Of *primary interest, however, will be how and when the DNS simulations depart from the equilibrium similarity solutions*. Unlike experimental data which are more limited, the DNS simulation results together with the theory will be seen to give considerable insight into how a turbulent flow develops from its initial conditions.

2. Basic Equations

The theory summarized below was presented in detail by George(1992). It begins with the spectral energy equation for isotropic turbulence given by:

$$\frac{\partial E}{\partial t} = T - 2\nu k^2 E \quad (2.1)$$

where $E(k, t)$ is the three-dimensional energy spectrum function defined by integrating the trace of three-dimensional spectrum tensor over spherical shells of radius $k = |\vec{k}|$. Similarity solutions were sought of the form:

$$E(k, t) = E_s(t)f(\bar{k}) \quad (2.2)$$

$$T(k, t) = T_s(t)g(\bar{k}) \quad (2.3)$$

where

$$\bar{k} = kl(t) \quad (2.4)$$

The functions $E_s(t)$, $T_s(t)$ and $l(t)$ were not assumed *a priori* as in the von Karman & Howarth(1938) and Batchelor(1953) analyses, but were determined from the equations themselves by an *equilibrium similarity* hypothesis described below. Substituting these into equation 2.1 and multiplying by $l^2/\nu E_s(t)$ yields:

$$\left[\frac{l^2}{\nu E_s} \frac{dE_s}{dt} \right] f + \left[\frac{l}{\nu} \frac{dl}{dt} \right] \bar{k} \frac{df}{d\bar{k}} = \left[\frac{l^2 T_s}{\nu E_s} \right] g - [2] \bar{k}^2 f \quad (2.5)$$

The *equilibrium similarity* hypothesis simply requires that the flow evolve asymptotically in time in such a manner that all of the terms in equation 2.5 retain exactly the relative value at the same value of scaled wavenumber \bar{k} . Said another way, all of the terms in square brackets of equation 2.5 must evolve with time in exactly the same way so the relative balance of the equation is maintained. Since one of them is constant, all must be. There is no reason to believe the constants to be independent of the initial conditions, nor are they.

The requirement for an equilibrium solution is precisely the requirement for any single set of scales to collapse the data over all wavenumbers, since the collapse can be perfect only if the equations admit to such solutions. *Why* the flow might behave this way has been a matter for speculation for nearly a century, but it has been generally observed that when such solutions exist, nature finds them, George(1989), (1999).

No further assumptions are required to determine the following:

- The **energy spectra** collapse at *all* wavenumbers *for fixed initial (or upstream conditions)* when plotted as $E(k, t)/u^2 \lambda$ versus $k\lambda$.
- The **non-linear spectral transfer function** collapses when plotted as $\lambda T(k, t)/\nu u^2$ versus $k\lambda$. This surprising result is the primary difference from the earlier analyses of von Karman & Howarth(1938), Batchelor(1953) and Lin(1961) who all *assumed* at the outset that T scaled with u^3 .
- The **turbulence energy** must decay as a power law:

$$\frac{3}{2}u^2 = B[t - t_o]^n \quad (2.6)$$

where t_o is a virtual origin and the exponent n is determined by the initial conditions. Note that this implies that the rate of dissipation is given by:

$$\epsilon = -\frac{3}{2} \frac{du^2}{dt} = -nB[t - t_o]^{n-1}. \quad (2.7)$$

- The **Taylor microscale** is given by:

$$\lambda^2 = \frac{10}{-n}\nu[t - t_o] \quad (2.8)$$

where

$$\lambda^2 \equiv 15\nu\frac{u^2}{\epsilon} \quad (2.9)$$

The linear dependence on time follows directly from the power law decay of the energy.

There are a number of immediate consequences of the above. Several are of interest here:

- The **Reynolds number** based on the Taylor microscale is given by:

$$R_\lambda = \frac{u\lambda}{\nu} = \left[\frac{20B}{-3n\nu}\right]^{1/2}(t - t_o)^{(n+1)/2} \quad (2.10)$$

George(1992) argues that $-5/2 < n < -1$, where these represent the zero and infinite source Reynolds number limits respectively. Hence in the limit of infinite Reynolds number, R_λ is constant during decay.

- **The integral scale** must be proportional to the Taylor microscale. This follows directly from the results above and its definition as:

$$L \equiv \frac{\pi}{2u^2} \int_0^\infty \frac{E(k, t)}{k} dk \quad (2.11)$$

The dependence of the denominator on k means that the integral scale is primarily determined by the lowest wavenumbers; hence how these are resolved will be of major interest. Also, note that $\epsilon L/u^3$ is constant *only* as the source Reynolds number becomes infinite ($n \rightarrow -1$).

- The **invariant** for the decay must satisfy

$$\int_0^\infty r^p B_{LL}(r, t) dr = I_p \quad (2.12)$$

where $B_{LL}(r, t)$ is the longitudinal correlation function and p is related to the energy decay exponent by:

$$p = -2n - 1 \quad (2.13)$$

The limits on n above correspond to $4 > p > 1$ where the last value corresponds to the infinite source Reynolds number limit. It is straightforward to show that equation 2.12 implies that the spectrum near zero wavenumber must be given by

$$E(k, t) = Ck^p \quad (2.14)$$

where C is a constant determined only by the initial conditions.

It is easy to show from equation 2.1 that $T(0, t) \equiv 0$ also.

- The **velocity derivative skewness** is given by:

$$S \equiv \frac{\langle (\partial u / \partial x)^3 \rangle}{[\langle (\partial u / \partial x)^2 \rangle]^{3/2}} \quad (2.15)$$

$$= -\frac{3\sqrt{30}}{14} \frac{\int_0^\infty k^2 T(k, t) dk}{[\int_0^\infty k^2 E(k, t) dk]^{3/2}} \quad (2.16)$$

It follows immediately from the results above for E and T that

$$SR_\lambda = \text{constant}, \quad (2.17)$$

but *only during decay for fixed initial conditions*. The constant appears to increase for increased source Reynolds number. It is obvious that if the resolution for k^2T is not as good as that of k^2E , then the computed results are not likely to confirm this relationship. It should be noted that similar relationships can be derived for all the normalized velocity and velocity derivative moments, so that the longer the turbulence decays, the more intermittent it will become. Hence R_λ cannot uniquely characterize the probability density function since both the source Reynolds number and the ‘‘age’’ of the turbulence matter.

Finally, there are a number of other implications of the theory which can be tested. For example, the enstrophy and palinstrophy spectral equations can be written as:

enstrophy

$$\frac{\partial}{\partial t}(k^2E) = k^2T - 2\nu k^4E \quad (2.18)$$

palinstrophy

$$\frac{\partial}{\partial t}(k^4E) = k^4T - 2\nu k^6E \quad (2.19)$$

The equilibrium similarity hypothesis applies equally to these equations and their integrals. Thus during decay for fixed initial conditions:

$$\frac{\int_0^\infty k^2Tdk}{2\nu \int_0^\infty k^4Edk} = constant \quad (2.20)$$

and

$$\frac{\int_0^\infty k^4Tdk}{2\nu \int_0^\infty k^6Edk} = constant \quad (2.21)$$

These particular ratios have the advantage that the quantities being compared are equally well-resolved (as is clear from the enstrophy and palinstrophy equations above), unlike the derivative skewness where the denominator is better resolved than the numerator. These direct consequences of the equilibrium similarity hypothesis can be contrasted with the classical idea of a *universal equilibrium range* of Batchelor(1953). For the latter the left-hand sides of equations 2.18 and 2.19 should be zero for wavenumbers above the energy-containing range, and the ratios of equations 2.20 and 2.21 should be unity.

3. The DNS data

Two simulations of isotropic turbulence will be used in the following sections: the simulation of Wray(1998) at CTR Stanford/Ames, and the simulation of Livescu *et al*(1999). They will be referred to respectively as Wray and LJM. The LJM simulation has been described in detail by the authors, and the details of the Wray simulation can be found in Jimenez *et al*(1993), so there is no need to repeat that information here. In brief, both were pseudo-spectral simulations. The Wray simulation used 512^3 Fourier coefficients which were truncated in k -space to 128^3 , while the LJM simulation was a 128^3 simulation. All raw data (including time) were non-dimensionalized (by the investigators themselves) with an arbitrary choice of velocity and length. This does not affect the similarity normalizations utilized here since these factor out, but it does mean that time and

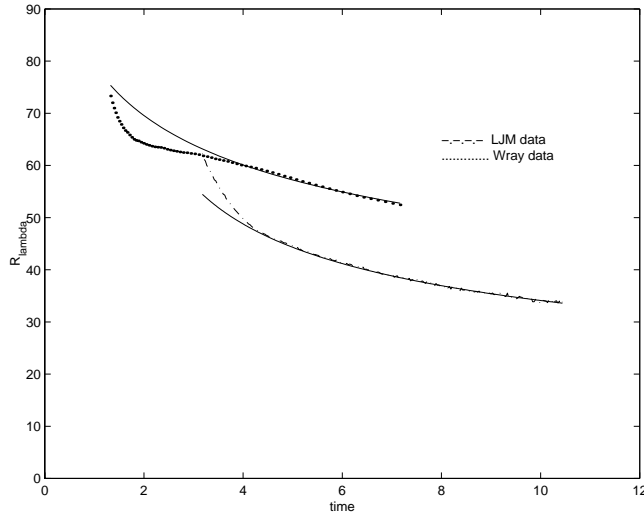


FIGURE 3. Variation of R_λ with time (Wray and LJM data).

other non-normalized variables (like u^2 and ϵ) from one simulation can not be directly compared to the other.

Both calculations were resolved to beyond the Kolmogorov microscale, and were carried out for very long times. The spectral codes used were quite similar, and the results differ almost entirely because of the initial conditions. These differences will be apparent in the presentations below, but were primarily due to the location of the peak in the initial energy spectrum which was at about $k = 6$ and 3 for the Wray and LJM simulations respectively. de Bruyn Kops & Riley(1998) have recently suggested the criterion $k_{min}L < 0.3$ (where L is the integral scale and k_{min} is the lowest wavenumber) in order to ensure negligible energy transfer from the lowest wavenumbers. For the Wray simulation, $k_{min}L \approx 0.2$, while for the LJM simulation $k_{min}L \approx 0.4$.

Figure 3 shows the variation of R_λ with time for both simulations. Also shown are the theoretical curves of equation 2.10 using the parameters of Section 5 below. The higher values of R_λ throughout decay for the Wray data are consistent with the slightly slower decay rate, as noted below.

4. The energy and dissipation spectra

Figures 4 and 5 show energy spectra from the Wray and LJM simulations normalized with u^2 and λ . Both linear-linear and log-log plots are shown. The collapse of the normalized plots makes it clear when the turbulence has reached an equilibrium similarity state. The high wavenumber tails are characteristic of numerically generated spectra, and mark the limits of resolution introduced by the averaging over spherical shells. Since the Kolmogorov microscale is increasing with time, the resolved portion of the high wavenumber spectra also increases with time. The normalized (and collapsed) plots for large times suggest strongly what the spectrum would look like for earlier times if the resolution had been better. They also suggest that for wavenumbers below the tail the simulations are indeed producing the correct values. The lowest wavenumbers will be discussed in Section 6 below, where it will be argued that the spectra are converging toward the lower values as time increases.

Figures 6 and Figures 7 show similar plots of $k^2 E$ for both sets of data. The Wray data

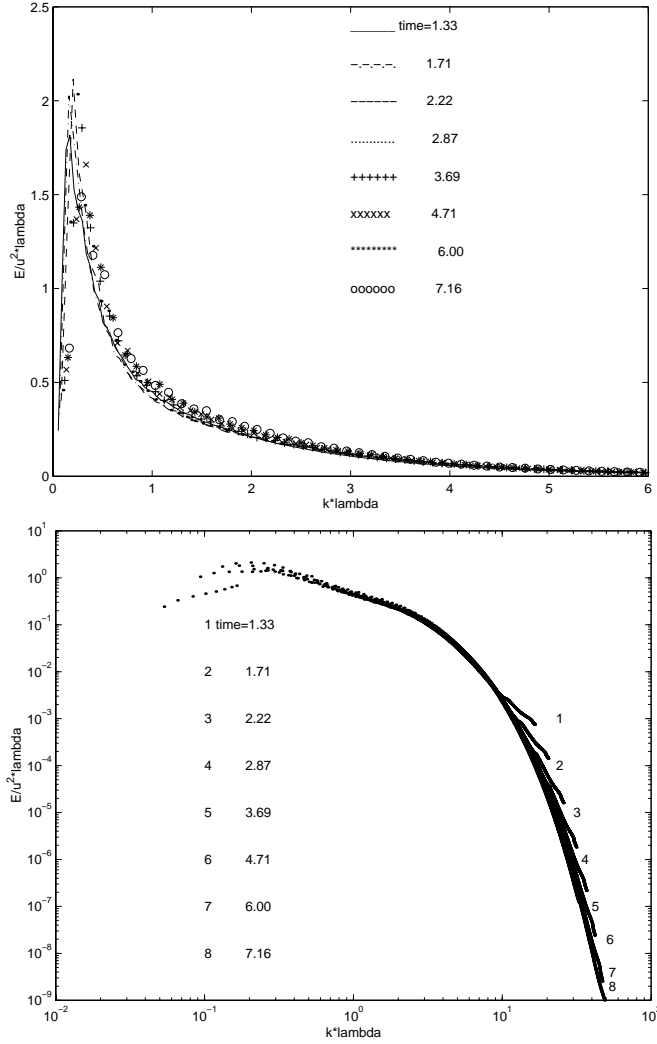


FIGURE 4. Energy spectra (Wray data).

were produced by first multiplying the spectral data by k^2 before averaging. Again the collapse over the resolved wavenumbers is remarkable. And as for the spectrum itself, the high wavenumber departures from a single curve can readily be recognized as being due to the averaging and resolution, since these move to progressively higher wavenumbers as the resolution improves with time.

5. The energy decay, dissipation and Taylor microscale

The spectral data can be directly integrated to obtain the energy, $3u^2/2$, and the dissipation, ϵ . The dissipation can also be determined from the time derivative of the energy. There was about a 5% difference between the two methods, at least past the initial transient. Figures 8 and 9 show the Taylor microscale (squared), energy and dissipation for the Wray data; the same plots for the LJM data are shown in Figures 10 and 11. Also shown are the power law decay curves using the parameters determined below.

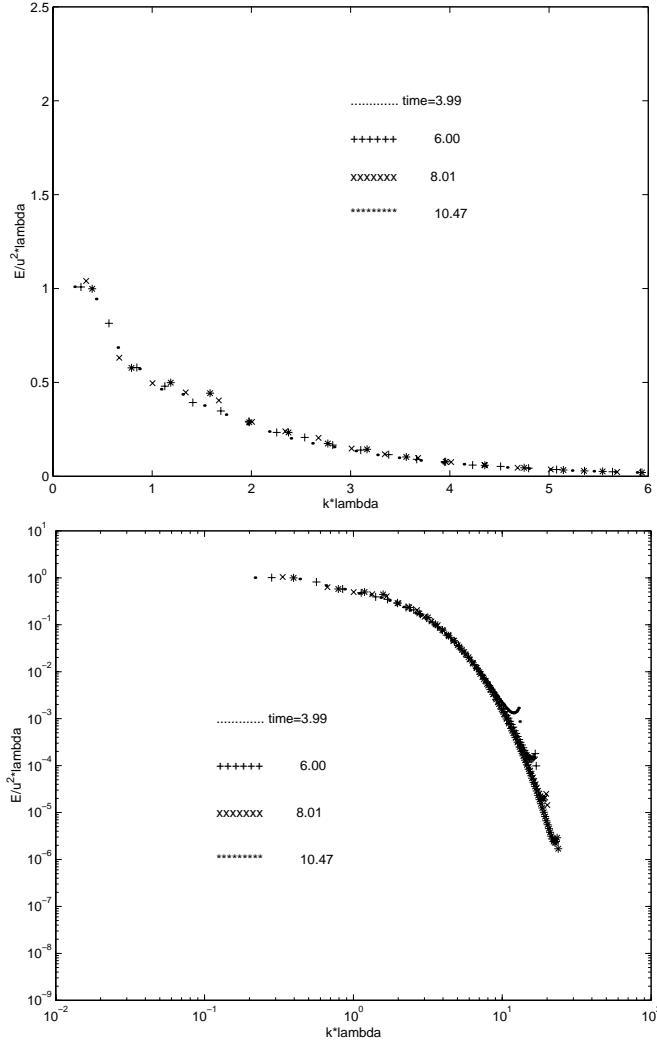


FIGURE 5. Energy spectra (LJM data).

The variation of the square of the Taylor microscale with time is the most interesting since the intercept of the best fit straight line with the time axis determines unambiguously the virtual origin. Unlike the energy decay where it is possible to fit various regions with a power law, there is little choice here as to which region is linear with time. Also, the very fact that λ^2 versus t is linear indicates that the energy is decaying as a power law as suggested in equation 2.8. Figures 9 and 11 also show plots of $(3u^2/2)^{1/n}$ and $\epsilon^{1/(n-1)}$ versus time. If the power has been correctly chosen and the decay is indeed a power law, then both of these curves should be linear in approximately the same range as the plot of λ^2 versus t . They clearly are.

A simultaneous regression fit to all three curves for $4 < t < 7$ yields the virtual origin in time for the Wray data as $t_o = -0.45$, the decay exponent as $n = -1.50$, and $B = 0.60$. The same procedure applied to the LJM data yields $t_o = +1.28$, $n = -1.61$, and $B = 3.03$. The constants showed only a very weak sensitivity to actual range of data

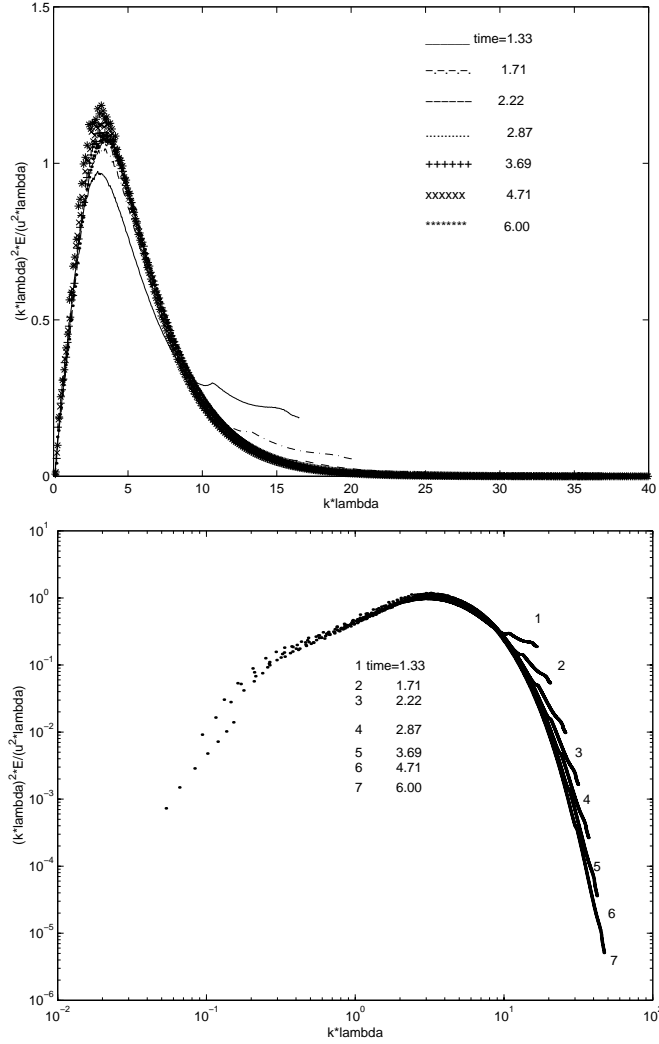


FIGURE 6. Dissipation spectra (Wray data).

used and to which curves were included in the optimization. The slightly higher decay exponent for the LJM data is consistent with the lower Reynolds number for this data.

6. The integral scale and the spectrum at very low wavenumbers

The theory requires that the integral scale (defined from the spectrum) and the Taylor microscale be proportional. This is a direct consequence of the fact that the spectra collapse with u^2 and λ . Figure 1 (presented in the Introduction) shows the ratio L/λ for the Wray and LJM data. It might be argued that this ratio is approaching a constant, but only very slowly. Clearly a careful inspection of the spectra at low wavenumbers is necessary.

From equation 2.11, the integral scale is defined by integrating $E(k, t)/k$ over all wavenumbers, which clearly weights the lowest wavenumbers. Figures 12 and 13 show the same spectral data above, but plotted as $[E(k, t)/k]/u^2 \lambda^2$ versus $k\lambda$. Note that since

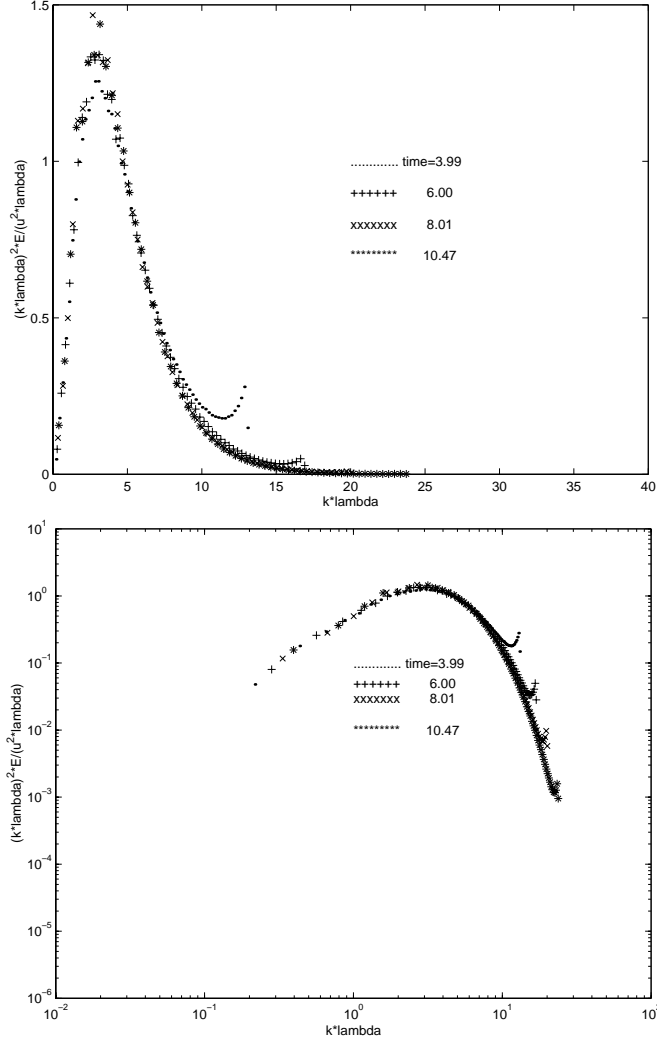


FIGURE 7. Dissipation spectra (LJM data).

$E(k, t) \rightarrow k^p$ as $k \rightarrow 0$ where $p > 1$, E/k must go to zero. This appears to be the case for the Wray data, but it is impossible to determine for the LJM data because there are no spectral estimates below the peak.

Although the Wray data collapse at all wavenumbers above about $k\lambda = 0.1$, there is clearly a lack of collapse at the very lowest wavenumbers. For these later times, say $t > 4$, the data appear to be approaching collapse for even the lowest wavenumbers. In fact, for the last two times the data are virtually identical. Unfortunately there are not many data points at the wavenumbers of most interest.

Some insight into the observed behavior at low wavenumbers can be obtained by considering the solution to equation 2.1, which can be written in terms of the initial spectrum as:

$$E(k, t) = E(k, t_o) \exp(-2\nu k^2[t - t_o]) + \int_{t_o}^t T(k, t') \exp(-2\nu k^2(t - t')) dt' \quad (6.1)$$

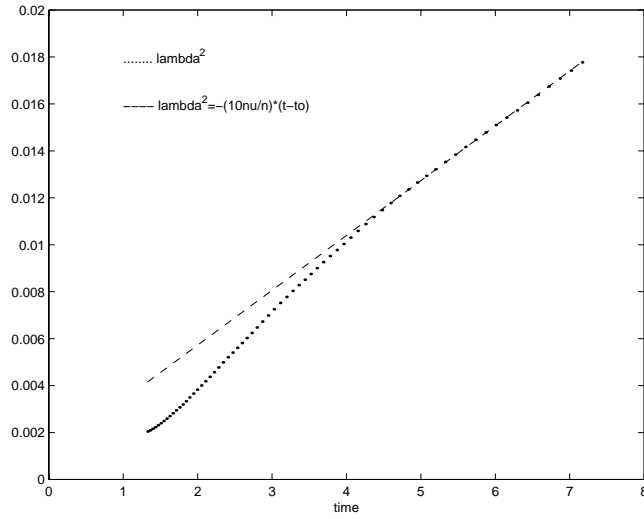


FIGURE 8. Taylor microscale (squared) as function of time (Wray data).

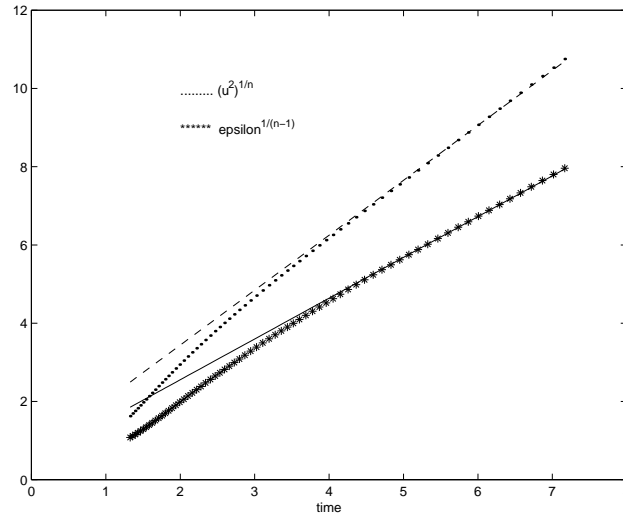


FIGURE 9. Energy and dissipation as function of time (Wray data).

It is clear from the first term on the right-hand side that no matter how large $t - t_o$ is, there is always a value of k below which the initial conditions persist. It is, of course, known how the calculation is started. Unfortunately because of the manner in which the turbulence is generated (usually from some random noise), it is not clear what the turbulence itself regards as its initial conditions; only that whatever they are, they will persist.

An alternative approach is to evaluate where and when the decay invariant of equations 2.13 and 2.14 apply. The decay exponent is -1.50 for the Wray simulation, so the corresponding value of p is 2.0 . Hence for the smallest wavenumbers, the theory requires $E(k, t) = Ck^2$ where $C = 24.8$ for these data. Figure 14 shows this curve together with the spectra at very low wavenumbers. Clearly the low wavenumber spectral data associ-

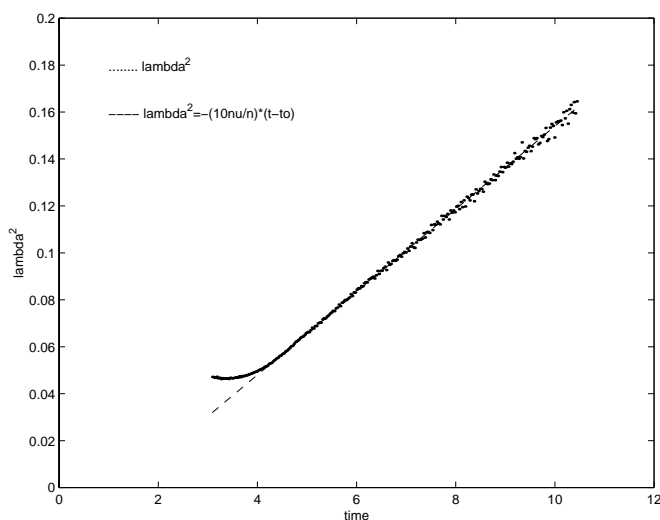


FIGURE 10. Taylor microscale (squared) as function of time (LJM data).

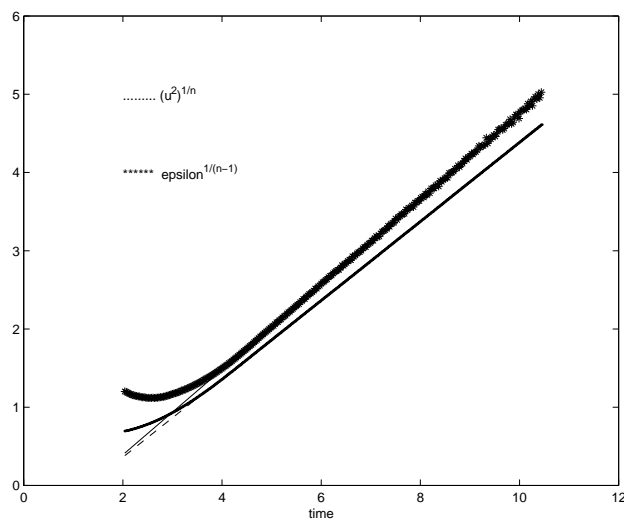
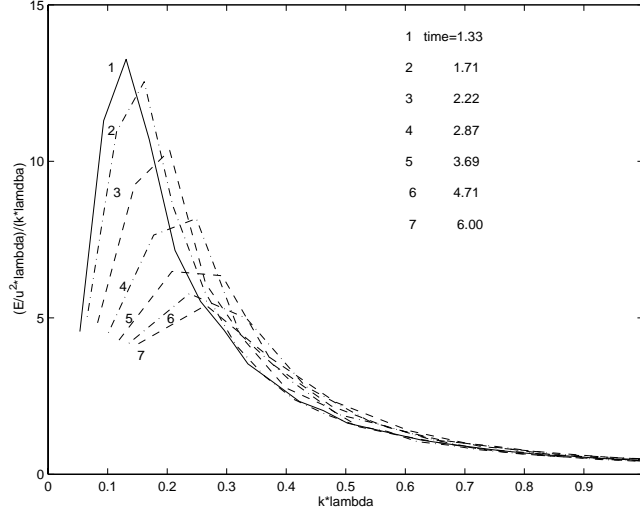
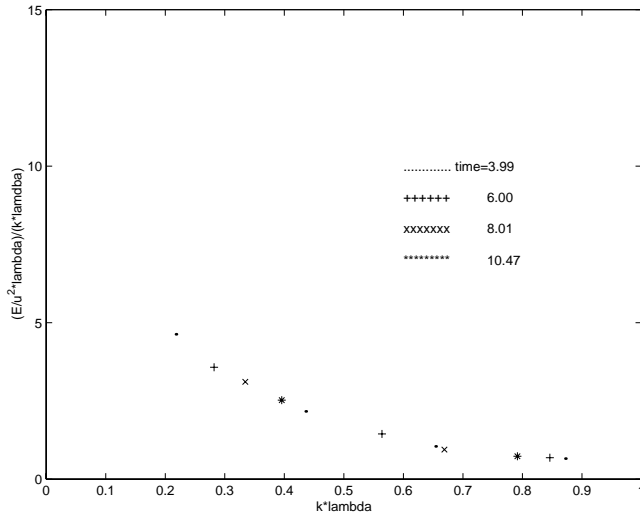


FIGURE 11. Energy and dissipation as function of time (LJM data).

ated from the early times is dropping toward this value, and appears to achieve it about the time the power law decay region identified above begins.

For the estimates of the integral scale for both sets of data, an interpolation function based on the zero wavenumber expansion was used to fill in the missing low wavenumber data. Even for the Wray data this contributes as much as 20% of the integral. Given the absence of the low wavenumber data, the estimates for the LJM data must be regarded as a lower bound.

In summary, both simulations taken together suggest that aforementioned problem with the integral scale is not a shortcoming of the theory. Even though the low wavenumbers were poorly resolved by the averaging, the normalized spectra are nearly collapsed there. The fact that the spectra at *all* wavenumbers collapse with u^2 and λ implies that

FIGURE 12. Blow-up of low wavenumbers for normalized $E(k, t)/k$ versus $k\lambda$ (Wray data).FIGURE 13. Blow-up of low wavenumbers for normalized $E(k, t)/k$ versus $k\lambda$ (LJM data).

$L/\lambda = \text{constant}$. And since the spectra themselves depend on the initial conditions, so must the constant. There is no evidence that the largest turbulence scales in either simulation have out-grown the computational domain, only that they have not reached equilibrium or were not resolved by the averaging.

The problems cited in the Introduction are thus more likely a consequence of using data for which the initial conditions have not died off, or of estimating the integral scale from calculations which did not contain enough data points to make a reasonable integration near the origin. In fact, the theory appears to provide a rather sensitive indication of the validity of the calculations at these low wavenumbers. In the future, a lack of collapse at these wavenumbers in these variables should certainly raise questions about whether the calculation has been carried out long enough.

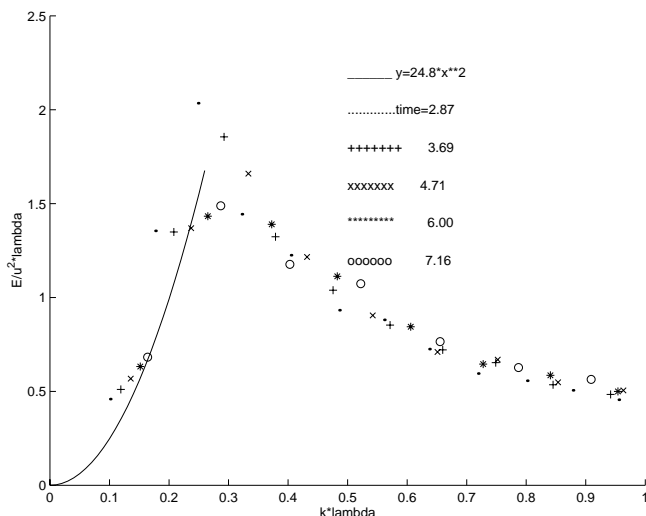


FIGURE 14. Blow-up of low wavenumbers for normalized $E(k, t)$ versus $k\lambda$ (Wray data).

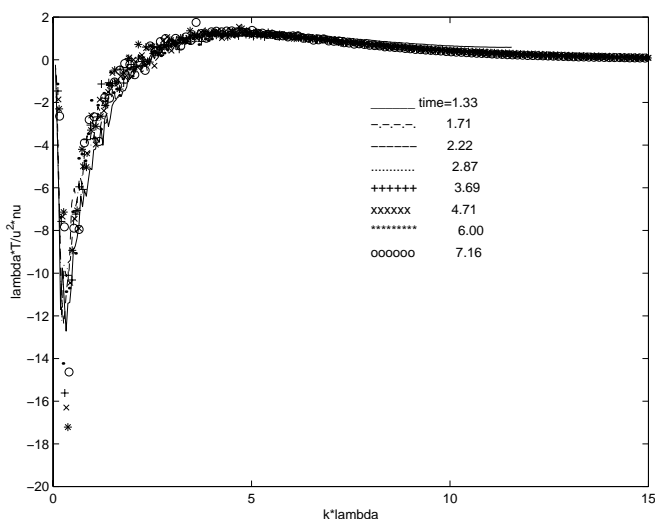
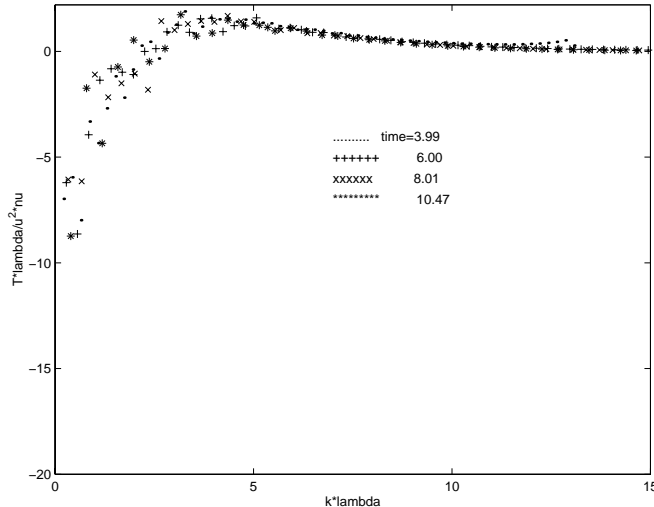


FIGURE 15. Normalized $T(k, t)$ versus $k\lambda$ (Wray data).

7. The spectral transfer

One of the most surprising features of the theory was the predicted scaling of the non-linear transfer terms. Figure 15 plots $\lambda T(k, t)/\nu u^2$ for the Wray data while Figure 16 shows the LJM data. The Wray data show remarkable collapse at all wavenumbers, as do the LJM data but with considerably more scatter.

The limitations of the DNS data at high wavenumbers are evident in Figures 17 and 18 which plot appropriately normalized versions of $k^2 T(k, t)$ and similarly normalized plots of $2\nu k^4 E(k, t)$ (which appear with $k^2 T$ in equation 2.18). Clearly the ability to accurately estimate these spectral moments improves as the resolution improves with time. And, as with the energy spectra themselves, even though the very high wavenumbers are compromised, those which are adequately resolved collapse as the theory suggests. Since it is the integral of $k^2 T$ which forms the numerator of equation 2.16, it is clear that

FIGURE 16. Normalized $T(k, t)$ versus $k\lambda$ (LJM data).

attempts to estimate the derivative skewness from these data will be very much in error, at least until the very end of the calculation. Both the sign and magnitude of the errors introduced by integrating a truncated k^2T are consistent with the departure of $-SR_\lambda$ from a constant, as shown in Figure 2 earlier.

On the other hand, the errors in these spectral moments at least contaminate the numerator and denominator of equation 2.20 and equation 2.21 the same way. Figures 19 and 20 plot these ratios as a function of time. The integrals were obtained by truncating the integration where the tail begins to deviate from the exponential roll-off. As suggested by the equilibrium similarity theory, these ratios rapidly achieve a constant value, in spite of the fact that both these moments are so poorly resolved over most of the calculations. Also, the ratios are less than unity, which confirms a failure of universal equilibrium at these Reynolds numbers.

Thus, in spite of the derivative skewness results, the collapse of the spectral and spectral transfer moments suggest strongly that the theory is an accurate description of these flows. The constancy of the ratios of integrals of the terms in the enstrophy and palinstrophy equations is direct confirmation of the validity of the equilibrium similarity hypothesis on which the theory is based. They also are consistent with the idea that the same principles can be applied to any order equation.

8. Summary and Conclusions

The results of this paper can be viewed in two ways: On the one hand it could be argued that the excellent agreement on all points between the theory and the DNS results confirms the validity of the theory. On the other hand it could be argued that the present results confirm the validity of the simulations, especially in light of the previously established agreement between experiment and theory.

In fact, both viewpoints are valid. The DNS results have been particularly useful in confirming that the theory indeed is valid at the largest scales, as well as for the integral scale. And the theory has been useful in helping to sort out the problems of resolution and aliasing in the simulations at the highest wavenumbers, especially their effect on such quantities as the derivative skewness. The theory has also provided a useful tool to

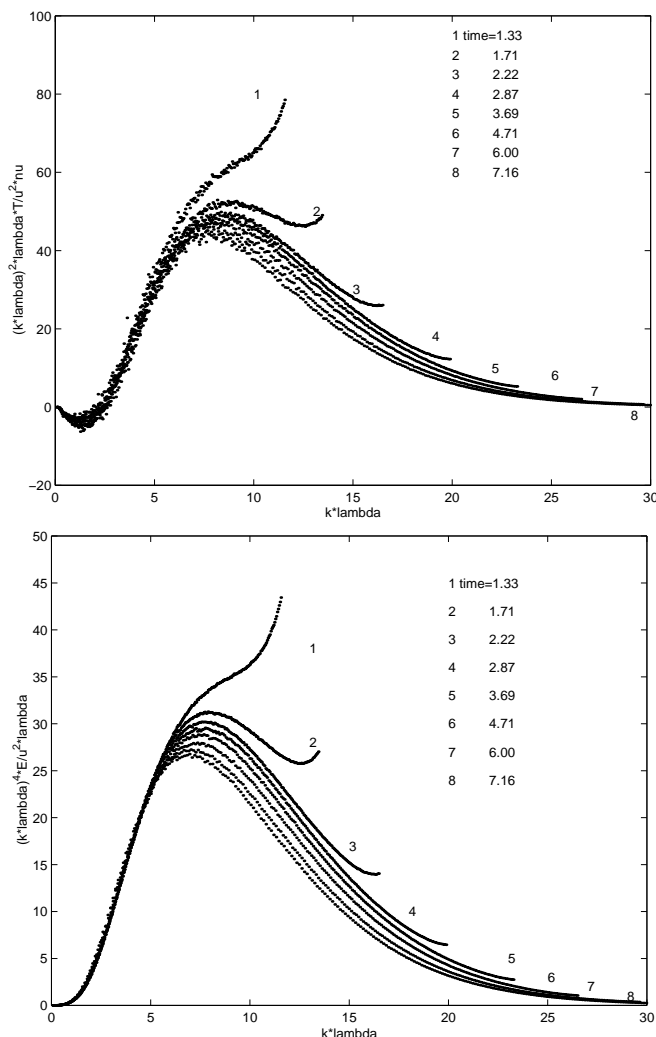


FIGURE 17. Normalized $k^2 T(k, t)$ and $k^4 E(k, t)$ versus $k\lambda$ (Wray data).

evaluate when the initial transient of the simulations can be considered to have died off at a particular wavenumber. As might have been expected, the larger scales take longer.

There are other implications of the new similarity theory which have not been explored here. This include: how the initial conditions affect the asymptotic state, the *increase* of intermittency during decay, and what are the implications for universality. Understanding the apparently separate (and opposite) roles of initial Reynolds number and local Reynolds number on the last two could be particularly helpful in interpreting the data. The results presented here suggest that perhaps the time has come when such investigations can produce meaning results, *but only if considerable care is taken to insure the data themselves are meaningful for the question under consideration*. Agreement with the equilibrium similarity theory would seem to provide a useful test, at least for decaying isotropic turbulence.

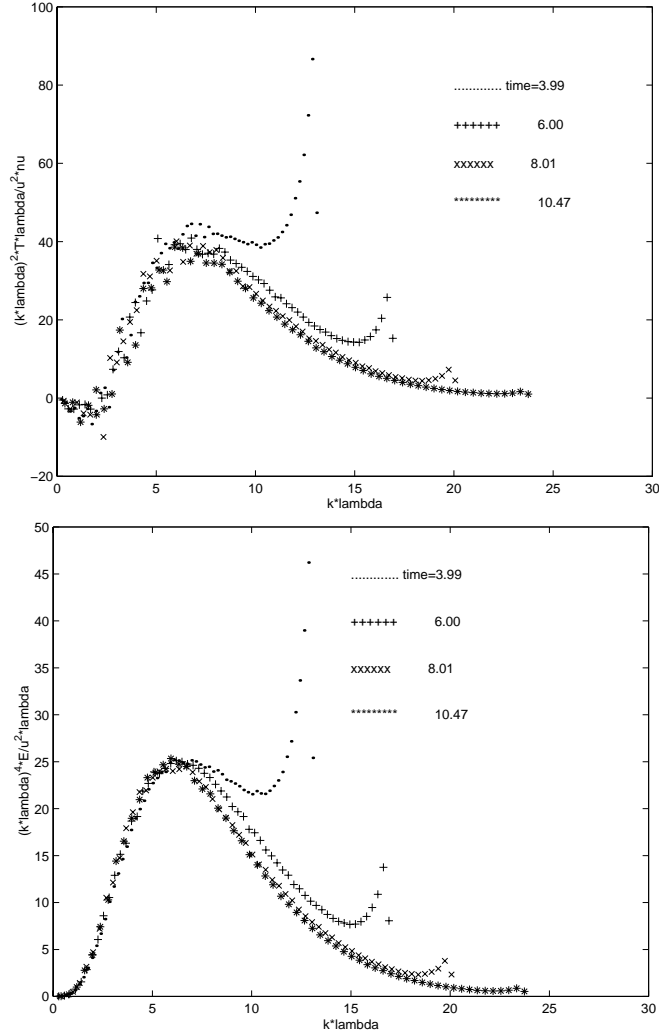


FIGURE 18. Normalized $k^2 T(k, t)$ and $k^4 E(k, t)$ versus $k\lambda$ (LJM data).

Acknowledgements

The authors are grateful to Alan Wray of NASA/Ames and to the Computational Fluids Laboratory of SUNY/Buffalo for making their DNS data available to us. The motivation for this study came from the intense discussions about turbulence at the Isaac Newton Institute for Mathematical Sciences of Cambridge University during the spring of 1999. WKG is especially grateful to Professors Keith Moffat and Christos Vassilicos for the opportunity to attend, and to the many participants for their interest and stimulating comments.

REFERENCES

- BATCHELOR, G. K. 1953 *The Theory of Homogeneous Turbulence*. Cambridge University Press, Cambridge, UK.
- DE BRUYN KOPS, S. & RILEY, J. 1998 Direct numerical simulation of laboratory experiments in isotropic turbulence. *Phys. Fluids* **10** (9), 2125–2127.

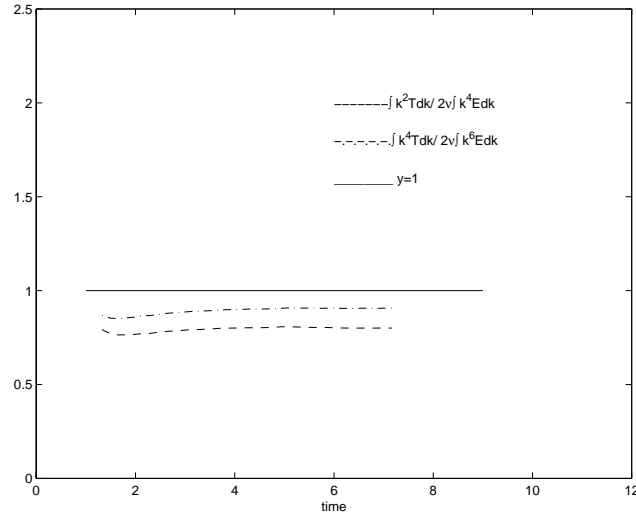


FIGURE 19. Ratios of equations 2.20 and 2.21 versus time (Wray data).

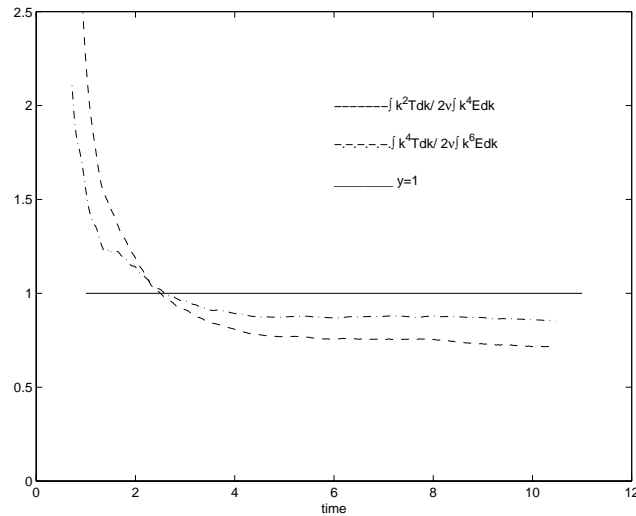


FIGURE 20. Ratios of equations 2.20 and 2.21 versus time (LJM data).

- COMTE-BELLOT, G. & CORRSIN, S. 1966 The use of a contraction to improve the isotropy of grid-generated turbulence. *Journal of Fluid Mechanics* **25**, 657–682.
- GEORGE, W. K. 1989 The self-preservation of turbulent flows and its relation to initial conditions and coherent structures. In *Advances in Turbulence*, pp. 39–73. Hemisphere, NY.
- GEORGE, W. K. 1992 The decay of homogeneous isotropic turbulence. *Physics of Fluids A* **4** (7), 1492–1509.
- GEORGE, W. K. 1999 Some thoughts on similarity, the pod, and finite boundaries. In *Fundamental Problematic Issues in Turbulence*, pp. 117–128. Birkhauser Verlag Basel/Switzerland.
- JIMENEZ, J., WRAY, A., SAFFMAN, P. & ROGALLO, R. 1993 The structure of intense vorticity in isotropic turbulence. *Journal of Fluid Mechanics* **255**, 65–90.
- VON KARMAN, T. & HOWARTH, L. 1938 On the statistical theory of isotropic turbulence. *Proc. R. Soc. Lond. A* **164**, 192.
- LIN, C. C. 1961 *Statistical Theories of Turbulence*. Princeton, NJ: Princeton University Press.

- LIVESCU, D., JABERI, F. & MADNIA, C. 1999 Passive scalar wake behind a line source in grid turbulence. *Submitted for publication* .
- WRAY, A. 1998 Decaying isotropic turbulence. In *AGARD*, pp. 63–64. Advisory Report 345.